

$L1_0$ FePt–MgO perpendicular thin film deposited by alternating sputtering at elevated temperature

Yingguo Peng,^{a)} Jian-Gang Zhu, and David E. Laughlin

Data Storage Systems Center, Carnegie Mellon University, Pittsburgh, Pennsylvania 15213

(Presented on 1 November 2005; published online 26 April 2006)

FePt–MgO two phase thin films have been obtained by an alternating sputtering method at elevated temperatures. It is found that the $L1_0$ FePt grains grow in a columnar manner through the thickness of the film and possess a (001) perpendicular texture promoted by the (200)-textured crystalline MgO underlayer. The amorphous MgO in the two phase mixture forms uniform separation walls between FePt grains. The microstructure is similar to that of Co-alloy/oxide granular media. © 2006 American Institute of Physics. [DOI: 10.1063/1.2176306]

INTRODUCTION

In pursuit of ultrahigh magnetic recording density, extensive studies have been performed on $L1_0$ FePt phase due to its high anisotropy field and good environmental stability. For perpendicular recording, the FePt thin films should consist of chemically ordered FePt grains with perpendicular (001) crystallographic orientation that are magnetically decoupled from each other. Unfortunately, the natural growth texture of FePt as-deposited films is (111) when it is deposited onto amorphous substrates because it forms in the fcc state. An underlayer with cubic symmetry and with (100) texture is needed to promote the perpendicular orientation of FePt. It is known that materials with the NaCl structure give rise to a (200) growth texture.¹ Among such materials MgO is widely used and has proven to be a good underlayer as it is readily grown with (200) texture.² MgO has a slightly larger lattice parameter than FePt, which is believed to be helpful to keep $L1_0$ FePt c axis perpendicular and reduce the in-plane variants ($a_{\text{MgO}} > a_{\text{FePt}} > c_{\text{FePt}}$). Also the good chemical stability and the high melting point of MgO are additional benefits since the FePt thin films must be ordered at high temperatures. In order to magnetically decouple the FePt grains, various materials (SiO_2 , MgO, C, B_2O_3 , BN, Si–N, AlN, etc) have been added into the FePt layer.^{3–7} It is desired that the added materials form uniform amorphous boundaries between the FePt grains. Figure 1 represents the typical microstructure of granular CoCrPt– SiO_2 perpendicular media, which is constructed with the plan-view and cross-section images in Ref. 8. However, a microstructure resembling that of Co-alloy/oxide granular media has not yet been reported in the FePt system. In this paper, we report on our efforts to develop FePt/MgO two phase films with similar microstructural features.

EXPERIMENT

Thin film depositions were carried out in a dc/rf sputtering tool with the base pressure of about 4×10^{-7} Torr and the argon flow for 5–10 mTorr. MgO thin films were deposited directly from an oxide target and FePt from an Fe target

mounted with Pt chips. The FePt composition was adjusted by changing the number of Pt chips and was finally fixed at about $\text{Fe}_{54}\text{Pt}_{46}$ in the thin films determined by energy dispersive x-ray fluorescence spectroscopy (EDXRF). The substrates used were mostly 1 in. Si wafers with native oxide for ease of transmission electron microscopy (TEM) sample preparation. Glass substrates were found to yield similar thin film microstructures. X-ray 2θ - ω scans were performed in both the out-of-plane and in-plane geometries at the psi tilt of 0° and 88° , respectively. In TEM observations, diffraction from the Si substrate was used to align the sample with the electron beam.

RESULTS AND DISCUSSION

It was found that a layer of amorphous Ta helps to grow better quality of MgO thin films with stronger (200) textures when deposited at room temperature. However, the texture was dramatically degraded when the deposition was done at elevated temperatures, presumably because Ta crystallized. As the result of x-ray 2θ - ω scans shown in Fig. 2, it was noticed that the 2θ value of MgO (002) peak shifted from 42.275° for the as-deposited film to 42.725° after heating to about 500°C for 30 min. The in-plane scans showed that MgO (200) peak also shifted to the higher angle, from 43.475° to 43.975° , by postannealing. This indicates that the MgO lattice shrinks in both the lateral and the vertical directions when it is heated up. It is also noticed that the lattice spacings are smaller in plane than along the normal direction even after heated to 500°C . This implies that MgO thin films have in-plane compressive stress even at the elevated

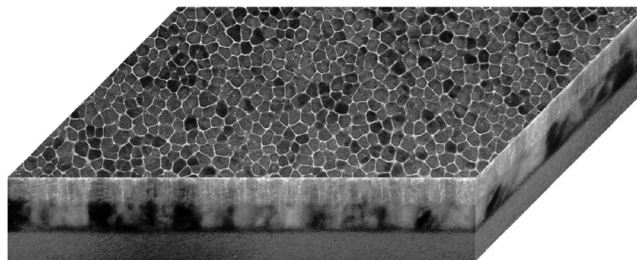


FIG. 1. 3D construction of TEM images of a CoCrPt– SiO_2 granular thin film, showing the desired microstructure for perpendicular recording.

^{a)}Electronic mail: yingguo@ece.cmu.edu

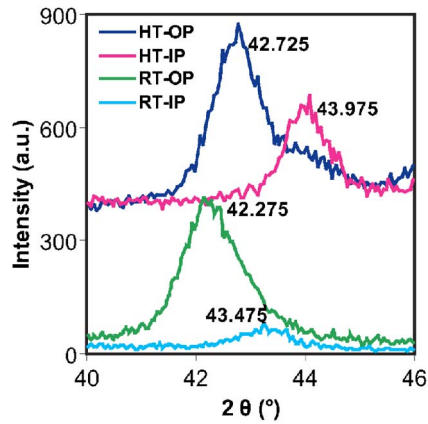


FIG. 2. (Color online) X-ray 2θ - ω scans of MgO as-deposited (RT) and postannealed (HT) thin films in in-plane (IP) and out-of-plane (OP) geometries.

temperature used for the FePt layer deposition. Since the MgO lattice is greater than that of FePt, the in-plane compressive stress in MgO reduces the mismatch between them and helps the cube-on-cube epitaxial growth of FePt. The dispersive angle [full width at half maximum (FWHM) of the rocking curve] of MgO (002) texture was measured to be about 6.4° , and that of FePt is about 7.2° . The similar FWHM values from the two layers indicate the existence of a good epitaxial growth of FePt on MgO.

In order to obtain the granular microstructure while retaining epitaxial relation between FePt and MgO, we employed a strategy of alternating sputtering of the ultrathin layers. First an ultrathin layer (<1 nm) of FePt was deposited onto MgO underlayer. The FePt forms heterogeneously as islands on top of the oxide MgO in the Volmer-Weber three-dimensional (3D) growth mode. Then an amorphous MgO was deposited to fill in the gaps between the islands. The amorphous MgO flattens on top of crystalline MgO underlayer in the Frank-van der Merwe two-dimensional (2D) growth mode. The next deposited FePt layer tends to form on the previous grown FePt islands when given adequate atom mobility. The process is repeated until the desired thickness is reached. The volume fraction of the two phase mixture is controlled by the ratio of the MgO and FePt thicknesses. It can be seen from TEM cross-section images (Fig. 3) that the lamella structure of (FePt 1 nm/MgO 0.5 nm) \times 6 almost remains when the FePt-MgO thin film is deposited at room temperature, while columnar FePt grains are present when the substrate is heated to 400°C . The inset electron diffraction pattern in Fig. 3 confirmed the epitaxial growth of FePt, in which the strong spots are from Si substrate and the vertical and horizontal streaks are from FePt. It should be pointed out that the ultrathin MgO between the FePt grains is amorphous and was deposited at different conditions than that of the crystalline MgO underlayer. The amorphous state was verified by the electron diffraction from the MgO capping layer deposited at the same condition, which is not shown here.

With the alternating sputtering deposition of FePt and MgO at elevated temperatures, a typical microstructure can be obtained as presented in Figs. 4(a) and 4(b). The signifi-

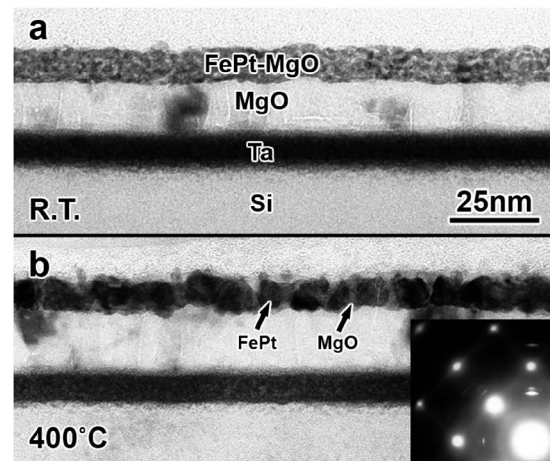


FIG. 3. TEM cross-section images of FePt-MgO thin films deposited at (a) room temperature and (b) 400°C . The inset electron diffraction pattern confirms epitaxial growth of FePt on MgO.

cant feature is that the amorphous MgO forms uniform boundaries with a thickness of $1\sim 2$ nm separating the FePt grains, although the FePt grains themselves do not form an equiaxed shape. When the deposition temperature was further increased, FePt grains with near equiaxed shape can be obtained by the complete separation of MgO boundaries, as shown in Fig. 4(c). Unfortunately, the grain size has also significantly increased at that high temperature of about

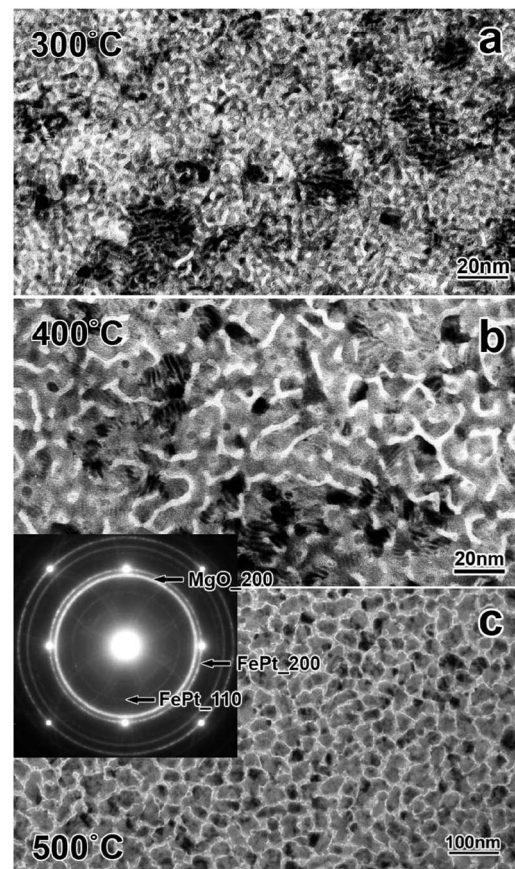


FIG. 4. TEM plan-view images of FePt-MgO thin films sputtered at different substrate temperatures. The (110) ring shown in the inset electron diffraction pattern indicates the chemical ordering in FePt deposited at 500°C .

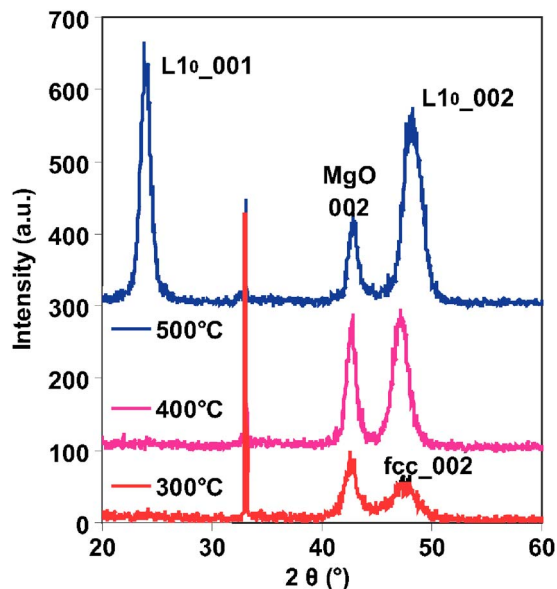


FIG. 5. (Color online) X-ray 2θ - ω scans of FePt-MgO thin films deposited at 300, 400, and 500 °C.

500 °C. A similar approach has been reported,⁹ but since the substrates were not heated for the whole deposition process, only a laminated microstructure was obtained.

The final microstructure is found to be affected by the thicknesses of FePt and MgO single layers and the substrate temperature. When the FePt single layer is too thick, the growth changed from Volmer-Weber mode to Stranski-Krastanov mode, and therefore the FePt grains cannot be well separated. On the other hand, when the FePt single layer is too thin, MgO layer has to be thin as well to maintain a certain volume fraction, and then the separation turned out to be poor too. In our experiments, 0.5–1 nm seemed to be a working range for FePt single layer thickness. Figure 4 demonstrated the microstructural change caused by the substrate temperature. With an increase of temperature, the FePt grains become larger, while the amorphous MgO separation wall remains relatively thin compared to the FePt grains. Also *in situ* chemical ordering has been observed at the substrate temperature of about 500 °C, as indicated by the (110) ring in the electron diffraction pattern (inset in Fig. 4).

X-ray diffraction scans of the FePt-MgO thin films deposited at different temperatures are displayed in Fig. 5. It can be seen that the FePt peak intensity increases with the substrate temperature, which corresponds to the increase of FePt grain size. At 500 °C, a strong (001) peak of FePt appeared as the result of the *in situ* chemical ordering. However, the (002) peak is noticeably much wider than (001), and its position is not exactly at the angle deduced from the (001) peak, but is slightly shifted to the lower side. This indicates that a (200) peak is hidden in the (002) peak, in other words, there are in-plane variants of $L1_0$ phase existing in the thin film. The order parameter is estimated to be about 0.7 by comparing the experimental I_{001}/I_{002} [after (002) peak deconvolution] with the theoretically calculated value. From Fig. 5 it is also seen that the MgO peak shifts to the higher angle, which means more compressive stress is released, with the increase of heating temperature.

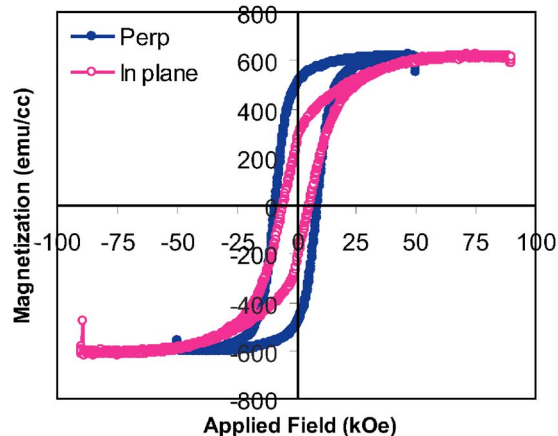


FIG. 6. (Color online) In-plane and perpendicular M - H loops of FePt-MgO thin film measured by PPMS.

Figure 6 displays the in-plane and perpendicular M - H loops of the FePt-MgO thin film sputtered at 500 °C measured by Physical Properties Measurement System (PPMS). The perpendicular and in-plane coercivities are about 8.7 and 5.5 kOe, respectively. The significant in-plane component shown in Fig. 6 confirmed the x-ray results about $L1_0$ in-plane variants. It should be pointed out that the in-plane variants can be more easily detected by magnetic measurements than by x-ray diffraction scans.

CONCLUSIONS

Perpendicular FePt-MgO thin films with a microstructure close to that of granular media have been obtained by the alternating sputtering method. Amorphous and crystalline MgO are successfully used to separate FePt grains and to promote perpendicular growth texture, respectively. However, more effort is needed to reduce the grain size and eliminate the in-plane variants of $L1_0$ phase. In addition, postannealing may be needed to obtain fully ordered $L1_0$ phase.

ACKNOWLEDGMENTS

The authors gratefully acknowledge Dr. Xiaowei Wu at Seagate Research for the PPMS measurement, and the Data Storage Systems Center at CMU and Seagate Research at Pittsburgh for their financial support on this project.

¹B. Lu and D. E. Laughlin, in *The Physics of Ultrahigh-Density Magnetic Recording*, Springer Series in Surface Sciences Vol. 41, edited by M. Plumer, J. Van Ek, D. Weller, and G. Ertl (Springer, New York, 2001), p. 45.

²S. Jeong, Y.-N. Hsu, M. E. McHenry, and D. E. Laughlin, *J. Appl. Phys.* **87**, 6950 (2000).

³T. Suzuki, H. Muraoka, Y. Nakamura, and K. Ouchi, *IEEE Trans. Magn.* **39**, 691 (2003).

⁴Z. Zhang, K. Kang, and T. Suzuki, *IEEE Trans. Magn.* **40**, 2455 (2004).

⁵J. A. Christodoulides, P. Farber, M. Daniil, H. Okumura, G. C. Hadjipanayis, V. Skumryev, A. Simopoulos, and D. Weller, *IEEE Trans. Magn.* **37**, 1292 (2001).

⁶M. L. Yan, H. Zeng, N. Powers, and D. J. Sellmyer, *J. Appl. Phys.* **91**, 8471 (2002).

⁷C.-M. Kuo and P. C. Kuo, *J. Appl. Phys.* **87**, 419 (2000).

⁸J.-G. Zhu, Y. Peng, and D. E. Laughlin, *IEEE Trans. Magn.* **41**, 543 (2005).

⁹R. Mukai, T. Uzumaki, and A. Tanaka, *IEEE Trans. Magn.* **39**, 1925 (2003).